KSME

Springer

Journal of Mechanical Science and Technology 37 (7) 2023

Original Article
DOI 10.1007/s12206-023-0601-8

Keywords:
· Moving load
· Complete ensemble empirical mode decomposition
· Power spectral density
· Intrinsic mode function
· Damage identification

Correspondence to:
Ying Zhang
yingzhang@hbu.edu.cn

Citation:
Fang, Y., Xing, J., Liu, X., Liu, D., Zhang, Y. (2023). Damage detection of bridge structures under moving loads based on CEEMD and PSD sensitivity analysis. Journal of Mechanical Science and Technology 37 (7) (2023) 3335~3346. http://doi.org/10.1007/s12206-023-0601-8

Received July 12th, 2022
Revised February 11th, 2023
Accepted March 8th, 2023

† Recommended by Editor No-cheol Park

Damage detection of bridge structures under moving loads based on CEEMD and PSD sensitivity analysis

Youliang Fang[1,2], Jie Xing[1], Xueting Liu[1], Danyang Liu[1] and Ying Zhang[1,3]

[1]College of Civil Engineering and Architecture Hebei University, Baoding, P.R. China, [2]Technology Innovation Center for Testing and Evaluation in Civil Engineering of Hebei Province, Baoding 071000, P.R. China, [3]Key Laboratory of Large Structure Health Monitoring and Control, Shijiazhuang 071002, P.R. China

Abstract This study proposes a new damage identification method based on a combination of complete ensemble empirical mode decomposition (CEEMD) and power spectrum density (PSD) sensitivity analysis to analyze the acceleration signals of bridge structures under moving loads and achieve damage detection of bridge structures. This paper has achieved the ability to accurately identify the location of cracks and the extent of the damage along a girder with only one acceleration sensor arrangement. The measured data is processed by the CEEMD method. The damage location is revealed by directly examining the first-order intrinsic mode function corresponding to the highest-order pseudo-frequency component, which presents an abrupt change at the damage location. Secondly, after determining the damage location of the bridge, only the power spectrum sensitivity analysis of the crack parameters at the damage location is required to obtain the damage level, avoiding the need to blindly solve the power spectrum for all elements. Finally, the identification method is validated by considering environmental noise, damage locations, and crack depths. The numerical simulation results and experiments for various working conditions show that the method adopted in this paper has good identification capability in identifying cracks in bridge structures.

1. Introduction

Long-term exposure of bridge structures to natural and man-made hazards may damage the structure over time or even cause sudden collapse. In order to avoid these unexpected events, it is particularly important to inspect bridge structures for early damage [1-4]. The presence of cracks reduces the bridge's local stiffness, but there is little or no change in the structure's intrinsic frequency. Changes in vibration patterns are more sensitive to local damage than changes in frequency. However, the detection of vibration pattern changes requires a large number of sensors [5, 6]. These reasons lead to the proposed damage identification method being hindered in practice [7]. In addition, the presence of cracks accelerates the corrosion of the structure by the external environment. Therefore, it is of great practical importance to study the damage identification of bridge cracks.

It is generally accepted that the abnormal changes produced by a damaged structure are hidden in the structural vibration data. Information on the damage to the structure can be obtained by processing the vibration data [8, 9]. Several signal processing techniques, such as wavelet variation and empirical modal decomposition, have been developed to uncover the damaged information in the response.

The response of a bridge structure under moving loads, which theoretically contains damage information of the whole bridge, suggests that damage detection of bridge structures can be achieved using fewer sensors [10]. Therefore, many scholars have taken the dynamic response of bridge structures under moving loads as the research object to explore the damage information hidden in the response. Yu et al. [11] combined the dynamic response of damaged bridges under moving loads with wavelet transform. They proposed using a wavelet coefficient

greyscale map and wavelet coefficient modal maxima trajectory map to identify the damage location. Zhu et al. [12] proposed wavelet analysis to identify the damage to bridge structures under moving loads and used the modal superposition method to analyze the dynamic characteristics of bridge structures under moving loads. Huang et al. [13] proposed a new signal processing method, the empirical modal decomposition method (EMD). This method has a better adaptive capability and does not require pre-set basis functions like wavelet transform, which has more potential in real-time signal processing [14].

Xu et al. [15] modelled the damage by reducing the stiffness of the first floor of a three story frame structure and identified the damage by empirical modal decomposition (EMD). Roveri et al. [16] used the Hilbert yellow transform to study the health state of a moving load through a girder bridge structure by applying the Hilbert transform to the intrinsic modal function corresponding to the first-order frequency of the bridge and by observing the first-order instantaneous frequency at the damage. By observing the crest of the first-order instantaneous frequency at the location of the damage, it was possible to identify the location of cracks in the bridge with just one sensor. However, one of the main problems of the EMD method is modal confusion. To suppress modal confusion, Wu et al. [17] proposed ensemble empirical mode decomposition (EEMD), which decomposes the original signal by adding different white noise several times and averaging the results of the multiple decompositions to obtain the final IMF. Aied et al. [18] used the EEMD method to analyze the acceleration response of a bridge under vehicular loading on a rough road surface. They identified the instant of change in bridge stiffness by IMF1, which can quickly identify the change in stiffness. To solve the problem that EEMD can change the amplitude and energy of the original signal when adding white noise, Yeh et al. proposed complete ensemble empirical mode decomposition CEEMD [19], which is an improvement of the decomposition techniques EEMD and EMD. Niu et al. [20] developed a combined data analysis method of Chebyshev filter (CF) and CEEMD for weakening the influence of the measurement noise. The results indicated that the global navigation satellite system and real-time kinematic (GNSS-RTK) technique were suitable for monitoring the dynamic response of large span bridges with reasonable accuracy by Chebyshev filter and complementary ensemble empirical mode decomposition (CF-CEEMD) analysis. In addition, the natural frequencies and modal modes of vibration experimentally derived by data-driven stochastic subspace identification the analysis were in good agreement with the predicted values based on the FE model.

Liberatore et al. [21] estimated the energy by power spectrum density analysis and analyzed the degree of structural damage using root mean square values, and applied it on a simply supported beam, where the energy in the bandwidth region most sensitive to the damage was combined with the modal vibration pattern, and the damage could be localized. Fang et al. [22] combined the power spectrum sensitivity method with the substructure reduction technique to achieve damage unit localization and damage degree identification of frame structures by measuring the partial degree of freedom response of the frame structures.

This paper proposes analyzing an acceleration signal on a bridge and performing an overall average empirical modal decomposition to obtain the highest order pseudo-frequency component generated by CEEMD, find the mutation's location and determine the damage location. After determining the location of the damage, a power spectrum sensitivity analysis is used to determine the crack depth at the location of the damage.

2. Methodology

2.1 Complete ensemble empirical mode decomposition (CEEMD) method

The EEMD algorithm adds white noise to the simple EMD decomposition so that the decomposed IMF is a single mode that optimizes mode mixing but introduces a new problem where the white noise does not cancel out completely after set averaging; there is residual noise, resulting in a reconstructed noise non-negligible. Therefore complete ensemble empirical mode decomposition (CEEMD) method is proposed [18]. The method reduces the residual amount of noise in the component data by adding n sets of the white noise of the opposite sign to the original signal to achieve negligible residual white noise, and the specific algorithm flow is shown below.

1) Add a pair of white noise signals with opposite symbols to the original signal. Two new signals are formed:

$$X_1^+ = x(t) + n_1^+(t) \tag{1}$$

$$X_1^- = x(t) + n_1^-(t) . \tag{2}$$

$\mathrm{n}_1^+(\mathrm{t})$ and $\mathrm{n}_1^-(\mathrm{t})$: the white noise signal with the same amplitude and opposite sign.

2) X_1^+ and X_1^- are decomposed by EMD to obtain the positive and negative noise integrated average of IMF^+ and IMF^-.

The final decomposition result is

$$IMF = (IMF^+ + IMF^-)/2 . \tag{3}$$

2.2 Power spectrum sensitivity

The full name of the power spectrum is power spectrum density (PSD), which refers to the signal power per unit frequency band. It is the most effective tool for studying random vibrations, transforming the original description of vibrations in the time domain into a description of vibrations in the frequency domain.

The dynamic equation for the forced vibration of a structure with multiple degrees of freedom is

$$M\ddot{X}(t) + C\dot{X}(t) + KX(t) = F(t) . \tag{4}$$

By converting the time domain to the frequency domain through the Fourier transform, we get

$$(K + iC\omega - \omega^2 M)X = F . \tag{5}$$

Then the frequency response function is

$$H_{(\omega)} = (K + iC\omega - \omega^2 M)^{-1} . \tag{6}$$

The power spectrum function is

$$S = H^* \cdot S_{ff} \cdot H^T . \tag{7}$$

2.2.1 Derivation sensitivity matrix

Based on the sensitivity of the structural damage identification method, the sensitivity matrix of the structural modal parameters or the dynamic response of the structure to the structural physical parameters is obtained first. Then the structural physical parameters changes are obtained according to the changes of the modal parameters or the dynamic response changes before and after the structural damage. The sensitivity is theoretically a derivative, such as the sensitivity of the response power spectrum of the structure to the structural crack depth is $\mathrm{S/d}$. In the case of fewer independent variables and matrix dimensions, it is relatively easy to obtain the function's derivative. However, for complex structures with many elements, finding the sensitivity directly by the derivative method is more difficult and sometimes even infeasible.

In this paper, the difference method is used instead of the derivative. The crack depth d is chosen as the damage parameter, while the crack depth is defined by setting the stiffness of the rotating spring k during the finite element analysis. S_i, S_0 represent the response power spectra of the corresponding structures in the damaged and undamaged cases, respectively. When there is damage of the structure, i.e., a small change in the initial crack depth d, the Taylor series expansion of S_i at d_0 is given by

$$\begin{aligned} S_i(d) &= S_0(d_0) + \sum_{j=1}^{n} \frac{\partial S_i}{\partial S_j} \Delta d_j \\ &+ \sum_{j=1}^{n} \sum_{k=1}^{n} \frac{\partial^2 S_i}{\partial^2 S_j} \Delta d_j \Delta d_k + \cdots \end{aligned} \tag{8}$$

By performing a first-order Taylor expansion for the damage parameters only and ignoring the higher-order terms, the above equation is written as

$$S_i(d) - S_0(d_0) = \sum_{j=1}^{n} \frac{\partial S_i}{\partial S_j} \Delta d_j . \tag{9}$$

In this paper, we apply the finite difference method. If the value of Δd is very small, it is considered that the derivative can be replaced by an approximation:

$$\frac{\partial S^A_{(\omega)}}{\partial d} \approx \frac{\Delta S^A_{(\omega)}}{\partial d} . \tag{10}$$

Assuming that there are m elements and n degrees of freedom in the simply supported beam, and assuming that the i-th element is damaged, a very small amount of damage Δd is taken, and the unit parameter matrix after the damage occurs is

$$d = [d_{01} \cdots d_{0i} + \Delta d \cdots d_{0m}]^T . \tag{11}$$

The power spectrum difference matrix is calculated as

$$\Delta S_{d(i)} = [S_{d(i)} - S_d|_p] \tag{12}$$

where, $S_{d(i)}$ is the response power spectrum of the i elements after the occurrence of damage. S_d is the response power spectrum without damage, and the subscript p represents the location of the measurement point. When there are more structural elements, the power spectrum matrix is calculated on a large scale. To decrease the calculation, the power spectrum values of k frequency point are selected to form a new sensitivity matrix. The sensitivity matrix of the response power spectrum variation $\Delta S^{(\omega)}_{d(i)}$ to the damage parameter d is expressed as follows:

$$\Delta S^{(\omega)}_{d(i)} / \Delta d = [(S^{(\omega)}_{d(i)} - S^{(\omega)}_d|_p) / \Delta d] . \tag{13}$$

Considering the calculated properties of the matrix, the power spectrum sensitivity matrix $\Delta S^{(\omega)}_{d(i)} / \Delta d$ is transposed.

To identify the damage degree, the elements in the power spectrum matrix need to be calculated differently for the damage parameters of each element. Because the damage location has been determined in the first step of this study, only the damage parameters at the damage location need to be calculated by difference.

$$\begin{bmatrix} \frac{S^{(\omega_1)}_{d(1)} - S^{(\omega_1)}_d|_p}{\Delta d} & \frac{S^{(\omega_1)}_{d(2)} - S^{(\omega_1)}_d|_p}{\Delta d} & \cdots & \frac{S^{(\omega_1)}_{d(m)} - S^{(\omega_1)}_d|_p}{\Delta d} \\ \frac{S^{(\omega_2)}_{d(1)} - S^{(\omega_2)}_d|_p}{\Delta d} & \frac{S^{(\omega_2)}_{d(2)} - S^{(\omega_2)}_d|_p}{\Delta d} & \cdots & \frac{S^{(\omega_2)}_{d(m)} - S^{(\omega_2)}_d|_p}{\Delta d} \\ \vdots & \vdots & \cdots & \vdots \\ \frac{S^{(\omega_k)}_{d(1)} - S^{(\omega_k)}_d|_p}{\Delta d} & \frac{S^{(\omega_k)}_{d(2)} - S^{(\omega_k)}_d|_p}{\Delta d} & \cdots & \frac{S^{(\omega_k)}_{d(m)} - S^{(\omega_k)}_d|_p}{\Delta d} \end{bmatrix} \begin{bmatrix} \Delta d(1) \\ \Delta d(2) \\ \vdots \\ \Delta d(m) \end{bmatrix} = \begin{bmatrix} S^{(\omega_1)}_{d(i)} - S^{(\omega_1)}_d|_p \\ S^{(\omega_2)}_{d(i)} - S^{(\omega_2)}_d|_p \\ \vdots \\ S^{(\omega_k)}_{d(i)} - S^{(\omega_k)}_d|_p \end{bmatrix} . \tag{14}$$

The resulting sensitivity matrix $\Delta S / \Delta d$ and the power spectrum difference $\Delta S^{(\omega)}_{d(i)}$ matrix form a set of super-static

equations, as shown in Eq. (14). By solving this system of super-stationary equations, the variables of damage parameters can be obtained, and structural damage identification can be realized.

2.2.2 Iterative steps of damage degree identification

After the response signal of the structure is obtained from the finite element analysis, the power spectrum function is calculated, and the sensitivity matrix is obtained from the response power spectrum before and after the structural damage. The sensitivity matrix can calculate the structural damage parameters obtained from the response power spectrum before and after the structural damage, and the whole iterative process is illustrated in Fig. 1.

As shown in Fig. 1, $S1$, $S2$ represent the response power spectrum functions of the structure before and after damage, respectively, $d1$ and denotes the initial crack depth matrix of the structure before the damage. In the figure, $\partial S/\partial d$ denotes the slope of the curve, and $\Delta S/(\partial S/\partial d)$ in the figure means Δd. The specific steps are as follows:

(a) Calculate the difference of damage parameters:

$$\frac{(S2-S(d))}{\partial(d)/\partial d1}=\frac{(S2-S(d))}{\Delta(d)/\Delta d1}=\Delta d1. \tag{15}$$

(b) The damage parameters are updated according to the difference $\Delta d1$ calculated in step (a) to get $d2=d1+\Delta d1$, and the PSD response function $S(d2)$ can be obtained.

(c) Judge whether the difference between $S(d2)$ and $S2$ satisfies the convergence criteria. Repeat steps (a) and (b) until ΔdN satisfies the allowable value set according to repeat steps (a) and (b) until satisfies the allowable value set according to the iteration precision and the convergence criterion is met.

2.3 Damage identification process

The existence of cracks will lead to the abnormal signal acquisition of bridge structure under vehicle load. However, the damage information of the bridge structure is hidden in the response signal, and the unprocessed acceleration signal cannot identify the bridge crack location. In this paper, a new method based on CEEMD and PSD sensitivity is proposed to detect the damage to bridge structures under moving load. This method uses a single-point measurement to accurately identify the location and depth of bridge cracks:

Step 1: The acceleration response is decomposed by CEEMD, and the damage location is determined from the highest-order pseudo-frequency.

Step 2: The sensitivity matrix of crack depth to power spectrum is constructed

Step 3: After the damage location is determined, the power spectrum matrix is reduced, and the rows and columns of the power spectrum matrix at the damaged element are selected. Finally, the damage degree is determined by an iterative method.

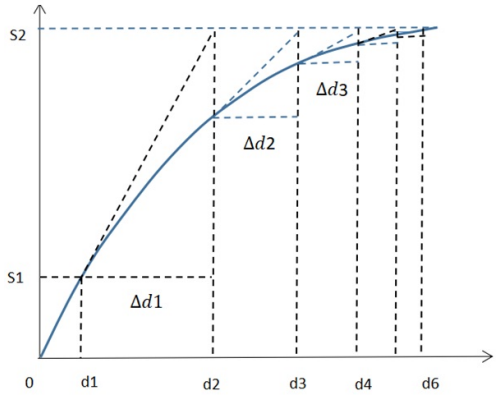

Fig. 1. Iteration process diagram.

3. Numerical studies

To evaluate the performance of the proposed technique in detecting structural damage in bridges, a simply supported bridge with physical geometric parameters is considered as beam length L = 20 m, section width and, height $b=h=$ 0.2 m; E = 2.0×10^{11} N/m^2; density ρ = 7800 kg/m^3; the magnitude of the moving load P = 1000 N and load speed V = 10 km/h. Where L_1 denotes the crack distance from the left end position. d denotes the crack depth.

The equation of motion of the beam can be expressed as

$$\rho A\frac{\partial^2 w(x,t)}{\partial t^2}+\frac{\partial^2}{\partial x^2}[EI(x)\frac{\partial^2 w(x,t)}{\partial x^2}]=P\Delta(x-x_p(t)) \tag{16}$$

and $x_p(t)=V_t$ represents the time history of the moving load while crossing the bridge.

The crack is located at L_1, and its depth is d. Also, the crack is modeled with a rotational spring, as shown in Fig. 2. According to the fracture mechanics theory [23], the stiffness of the rotational spring is defined as k:

$$k=1/\phi \tag{17}$$

$$\varphi=\frac{2h}{EI}(\frac{\delta}{1-\delta})^2(5.93-19.69\delta+37.14\delta^2-35.84\delta^3+13.12\delta^4) \tag{18}$$

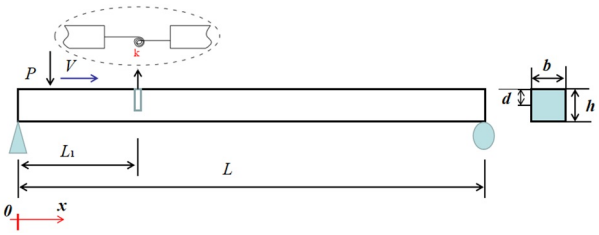

Fig. 2. Simply supported beam with an open crack, subject to a moving load.

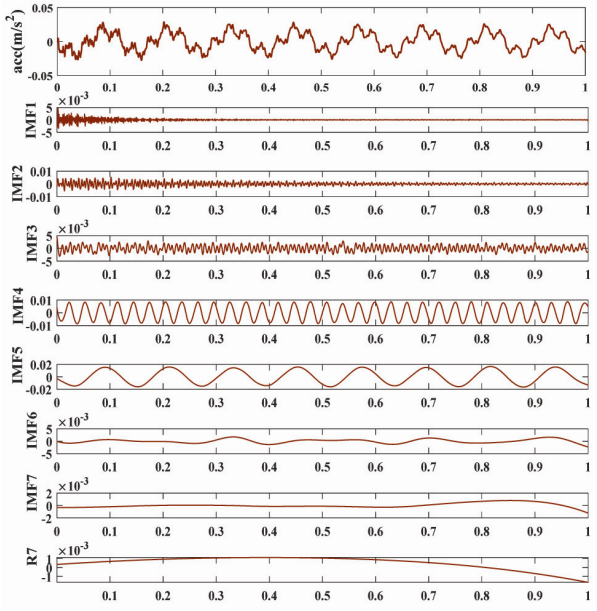

Fig. 3. CEEMD decomposition of health acceleration signal.

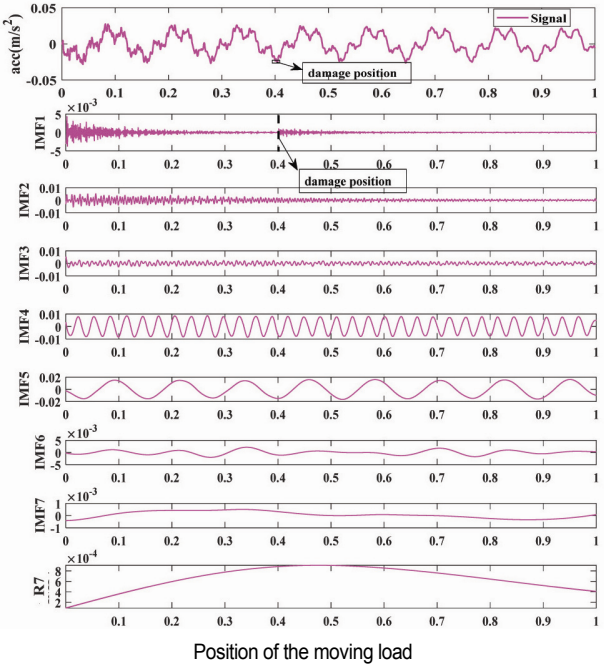

Fig. 4. CEEMD decomposition of acceleration signal at damage state ($L_1 = 0.4\,L$ and $d = 0.4\,h$).

where $\delta = d / h$ is the ratio of the crack depth d to the height of the beam.

3.1 No ambient noise identification

3.1.1 Single damage identification

As shown in Fig. 3, the acceleration signal in the undamaged state is decomposed by the CEEMD method into eight components, of which the last one is a residue. The decomposed IMF1-IMF7 is arranged successively from high frequency to low frequency. IMF1 is a pseudo-frequency component. The location and depth of the crack are chosen as follows: L_1 = 0.4 L; d = 0.4 h in Fig. 4. The unprocessed acceleration response does not directly determine the damage information of the structure. Using the proposed method, the acceleration response of bridge structure at 5/16 position under moving load is processed by CEEMD method, and IMF1-IMF7 and a residue (R7) are also obtained. Comparing Figs. 3 and 4, we can see that the acceleration signal of the damage state is decomposed by CEEMD, where the highest order pseudo-frequency component, IMF1, produces an abrupt change at the damage location. The undamaged state acceleration signal decomposition result in IMF1 does not have this abrupt change at the damage location in Fig. 3.

Comparing Figs. 4 and 5, it can be found that as the damage degree increases, the sudden change of IMF1 at the damage location becomes more obvious. Higher order frequency is more sensitive to the damage, so the highest order pseudo-frequency (IMF1) will be selected as the feature signal for damage location identification afterwards. As the damage degree increases, the change in the magnitude of the intrinsic mode function at the damage location can be used to identify

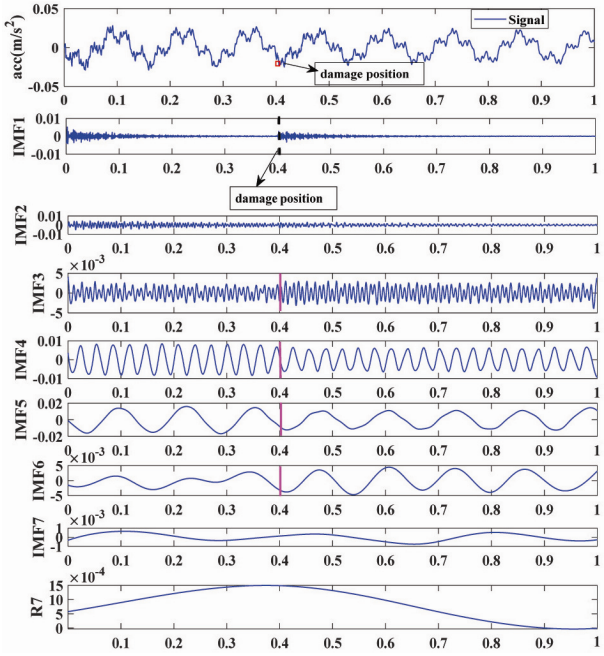

Fig. 5. CEEMD decomposition of acceleration signal at damage state ($L_1 = 0.4\,L$ and $d = 0.6\,h$).

the damage location in the low-order IMF.

3.1.2 Damage degree identification

The sudden change of IMF1 position has identified the damage location. Next, the degree of damage is identified using the

power spectrum sensitivity method. Because the damage location has already been identified, we only need to find the power spectrum sensitivity part of the rows and columns related to the damage location. Fig. 6 shows the acceleration power spectrum response curve. The frequency of the structure can be obtained from the peak of the power spectrum curve. As can be seen from the curves, the power spectrum function is different before and after the damage, which also indicates that the power spectrum function can characterize the damage.

The frequency range ω = 40-45 Hz is chosen. The sensitivity of the power spectrum to the depth of the fracture is obtained in Eq. (13). Then the damage parameters of the structure after damage are calculated by Eq. (14). After 12 iterations, the damage identification results are obtained as shown in Fig. 7, and the two figures show that the single damage degree of the structure can be successfully determined. The detection error is 1.25 %.

Fig. 8 shows the identification results and iteration results for a damage degree of 0.6 h. It can be seen that after 14 iterations, the damage degree of 0.59 h is finally identified accurately. The detection error is 1.67 %.

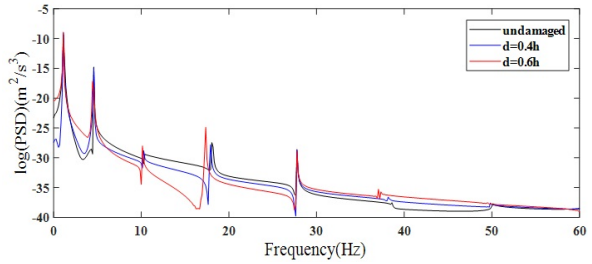

Fig. 6. PSD curve of measurement point at 5/16 L under single damage condition $L_1 = 0.4\,L$.

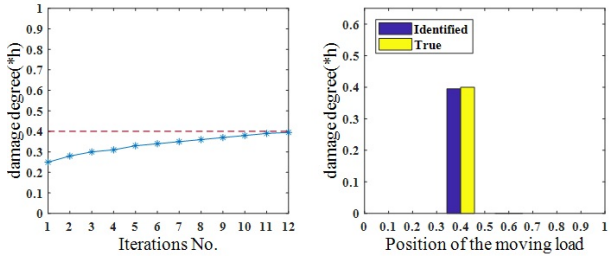

Fig. 7. The damage identification results for the damage degree of 0.4 h.

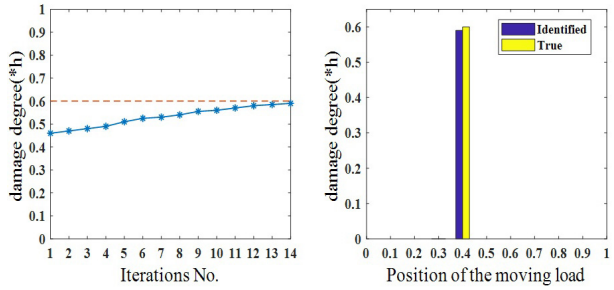

Fig. 8. The damage identification results for the damage degree of 0.6 h.

3.1.3 Multiple damage identification

The damage is assumed to occur at $L_1 = 0.4\,L$ and $d = 0.4\,h$; $L_1 = 0.75\,L$ and $d = 0.3\,h$. The damage locations are identified by direct detection of the highest order pseudo-frequency component (IMF1), which exhibits mutations at the damage locations. As shown in Fig. 9, using the proposed method in this paper, multiple damage locations can be accurately identified.

The corresponding acceleration power spectrum response curves are made as shown in Fig. 10, and it can be seen from the graphs that the power spectrum functions are different before and after the damage, which also indicates that the power spectrum functions can characterize the damage to the structure. The frequency range ω = 4.9-5.4 Hz is selected to identify the damage. After 15 iterations, and the damage identi-

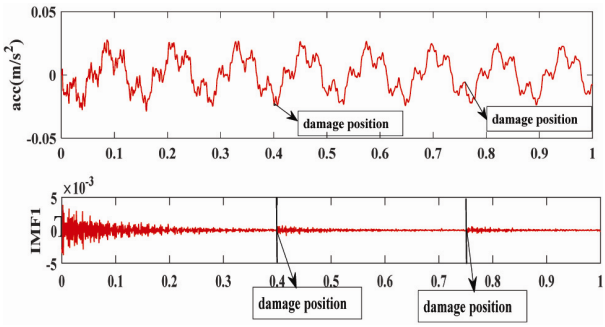

Fig. 9. Multiple damage identification.

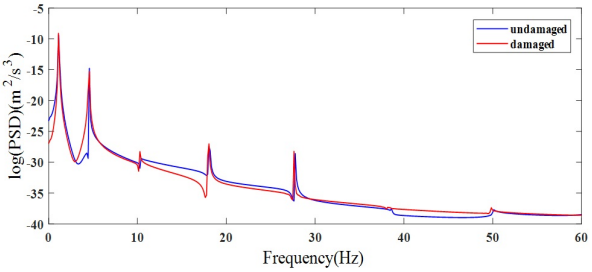

Fig. 10. PSD curve of measurement point at 5/16 L under multiple damage condition.

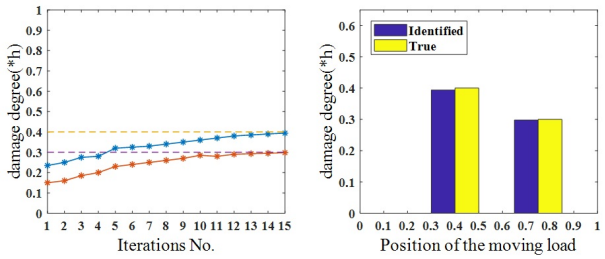

Fig. 11. Identification results of multiple damage.

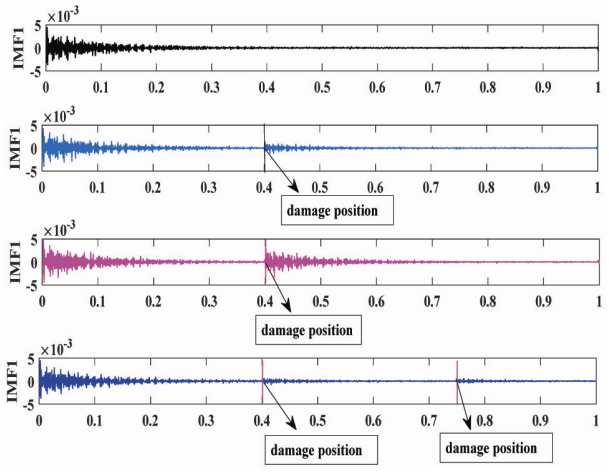

Fig. 12. Damage location identification results (SNR = 45).

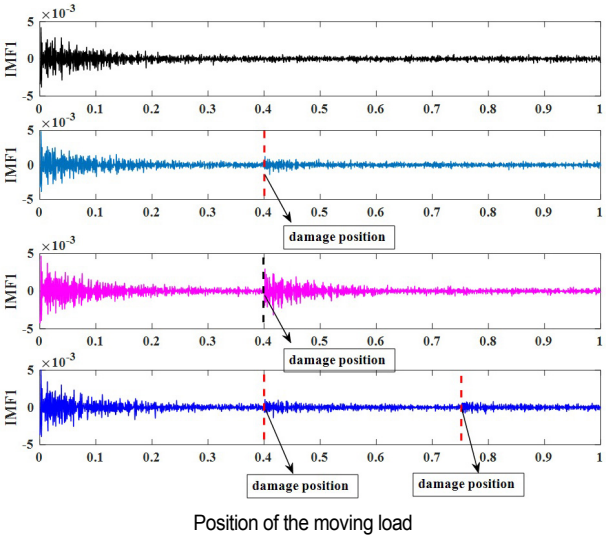

Fig. 13. Damage location identification results (SNR = 34.25).

fication results are obtained shown in Fig. 11, and the damage degree occurred at L_1. This figure shows that the multiple damage of the structure can be successfully identified by damage quantification. There is no misidentification phenomenon, and the maximum error of damage element detection is 1.5 %. The simulation example shows that this method can successfully detect multiple damages to the structure.

3.2 Effect of ambient noise

In vibration tests, ambient noise is inevitable, and noise can cause errors in the model analysis results. SNRS of different sizes are added to the original acceleration response to consider that the proposed method is not affected by environmental noise, while other parameters remain unchanged so that the robustness of the proposed method to noise can be evaluated.

$$SNR = 10\log_{10}\frac{P_s}{P_n}dB\ . \tag{19}$$

P_s - The power of signal; P_n - The power of noise.

As shown in Fig. 12, the first sub-image represents the identification result of undamaged; the second sub-graph shows the identification result of the damage location at 0.4 L and the damage degree of 0.4 h; the third sub-graph shows the identification result of the damage location at 0.4 L and the damage degree of 0.6 h; the fourth sub-graph shows the identification results of the damage location at 0.4 L and 0.75 L, and the damage degree of 0.4 h and 0.3 h respectively. It can be seen that in the case of SNR = 45, IMF1 can still accurately identify the location of cracks by sudden changes in the damage location. Compared with the second sub-graph and the third sub-graph, it can also be seen that with the increase of the damage degree, the sudden change in the damage location becomes more obvious. As shown in Fig. 13, for the recognition results

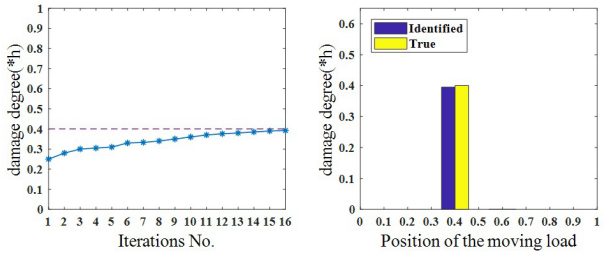

Fig. 14. SNR = 34.25, single damage identification ($L_1 = 0.4\ L$; $d = 0.4\ h$).

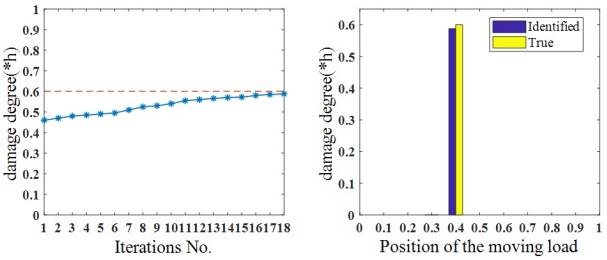

Fig. 15. SNR = 34.25, single damage identification ($L_1 = 0.4\ L$; $d = 0.6\ h$).

when SNR = 34.25 is added, the damage location can still be identified using the proposed method even in the case of large noise. Comparing Figs. 12 and 13, it can be found that with the increase of noise, there are also small mutations at the undamaged location, but the mutation at the damaged location is large, and the damage location can still be identified.

In a single damage condition, the crack depth at the damage element is solved by iteration using the power spectrum sensitivity method, and after 16 iterations, the iterative results and the iterative process are shown in Fig. 14. The identified damage degree is 0.391 h, and the identification error is 2.25 %; similarly, as shown in Fig. 15, after 18 iterations, the identified damage degree is 0.585 h, and the identification error is 2.5 %. Compared with the identification error without adding noise, it

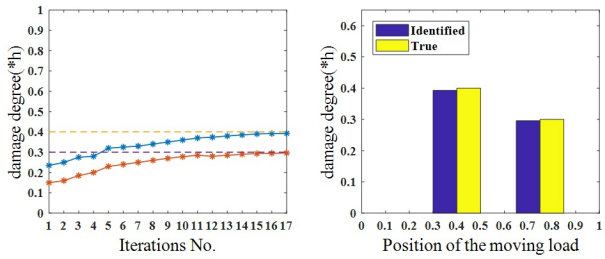

Fig. 16. SNR = 34.25, multiple damage identification.

shows that the identification accuracy decreases after adding noise, but the quantitative analysis of damage identification can still be carried out within a certain error allowance.

As multiple damage locations have been identified, the power spectrum sensitivity analysis is used to solve parameters at the damage locations only by iteration, and the iterative results and iterative process are shown in Fig. 16. The damage degree of the identified structure is 0.392 h and 0.293 h, respectively, and the maximum identification error is 2.33 %. Under the noise interference, the identification accuracy of the method is decreased, but the damage quantification can also maintain a certain accuracy, which can achieve better identification results, indicating that the method of this paper has certain noise resistance performance.

4. Experimental study

An experimental study was conducted on a simply supported aluminum beam (Fig. 17) to investigate the effectiveness and efficiency of the proposed based on CEEMD and PSD sensitivity analysis identification method. The plane view, cross section and dimensions of the aluminum beam are shown in Fig. 17(b). The beam has a uniform cross section of 120×20 mm (width× thickness), modulus of elasticity of E = 7.3E10 N/m^2, and density of 2750 kg/m^3.

A two-axle vehicle with four wheels was used for the test. Five sensors were installed on the bridge to record acceleration response. An opening of 5 mm in depth was cut in the mid-span of the beam to simulate a crack. Then, the vehicle was driven by the tractor to pass the beam at a uniform speed of 1 m/s.

To better investigate the bridge frequency and CEEMD decomposition ability, first, a sensor signal under random excitation for a period of time was randomly selected, as shown in Fig. 18(a). The power spectrum analysis of the collected acceleration signal gives the curve, as shown in Fig. 18(b), and the first 5 frequencies of the bridge can be seen from the curve.

The acceleration signal is decomposed by CEEMD, as shown in Fig. 19, to study the frequency of each component, The decomposition is not complete, but the corresponding bridge frequency per IMF can be seen. Fig. 20 is the power spectrum curve from IMF1. The IMF1 corresponds to the fourth to sixth-order frequencies of the bridge, as shown in Fig. 19. IMF2 and IMF3 are 21.75 Hz, corresponding to the second frequency of the bridge. Both IMF4 and IMF5 are 5.63 Hz for

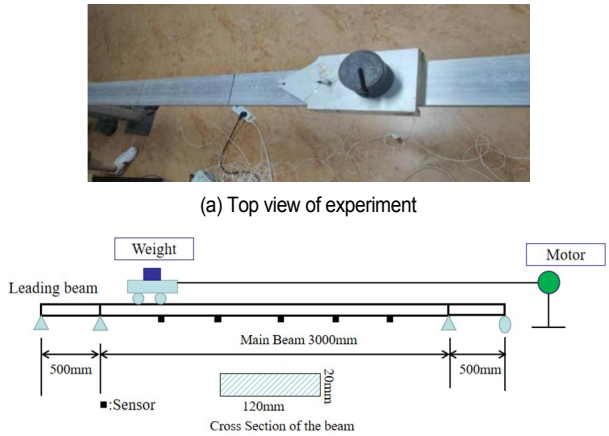

(a) Top view of experiment

(b) Arrangement and configuration of the experimental beam

(c) Overall view of the experiment

Fig. 17. Experimental arrangement and testing.

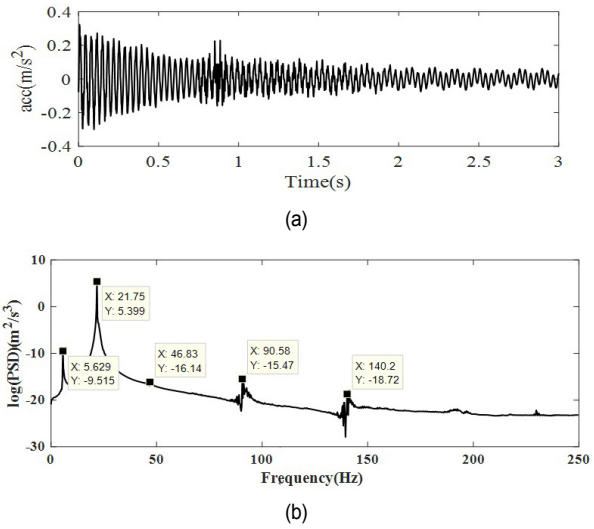

(a)

(b)

Fig. 18. (a) Sensor no. 4 acceleration signal; (b) PSD curve.

the first frequency of the bridge.

Fig. 21 is the acceleration signal of the vehicle passing through the damaged bridge at the speed of 1 m/s, 1/3 span (sensor no. 2). The acceleration response obtained from the collection is decomposed to obtain as shown in Fig. 22. IMF1 contains considerable noise because of the friction of the car

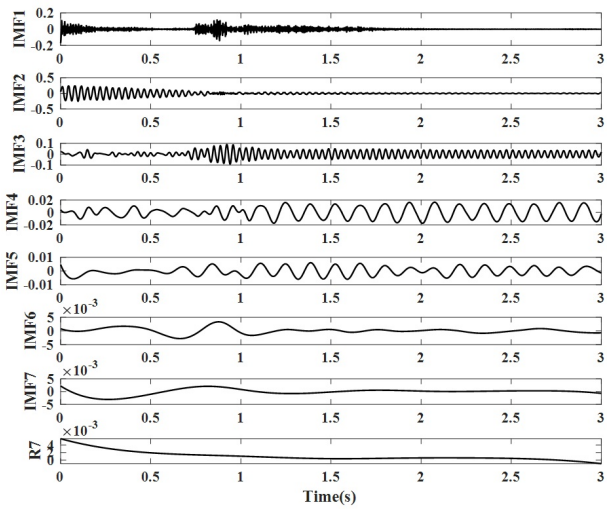

Fig. 19. CEEMD decomposition of acceleration signal.

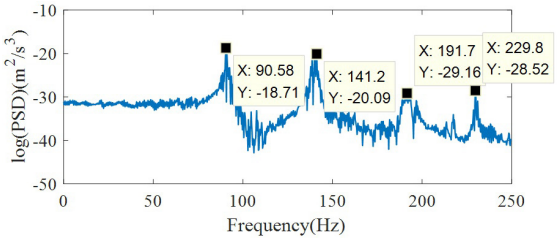

Fig. 20. IMF1 corresponding to PSD curve.

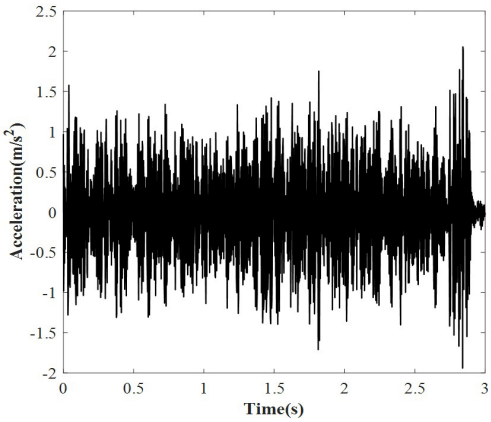

Fig. 21. Sensor no. 2 acceleration signal.

as it moves and because the actual signal acquisition itself is more complex than the numerical simulation. Therefore, the IMF1 is decomposed again and filtered to select the signal near the fourth-order frequency for study, as shown in Fig. 23. In particular, the IMF1 signal changes obviously when the car reaches the damage position, and the instantaneous amplitudes of IMF2-IMF5 and R7 suddenly change downwards at the damage position, resulting in a trough. This also indicates that the damage occurred near the middle of the bridge span.

Fig. 24 shows that there is an abrupt change in the signal at

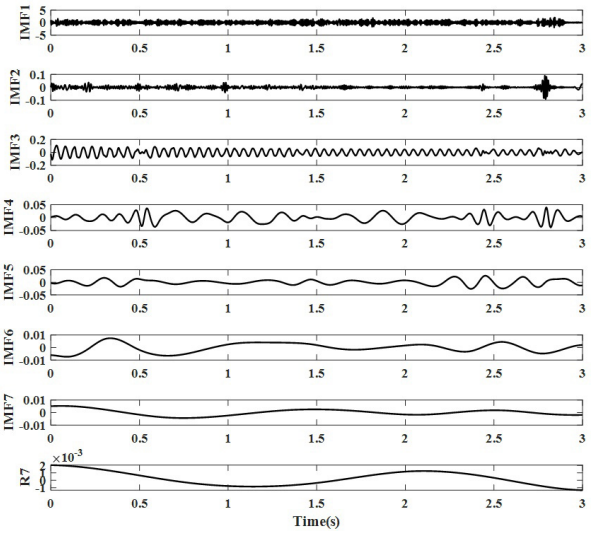

Fig. 22. CEEMD decomposition of acceleration signal at damage state.

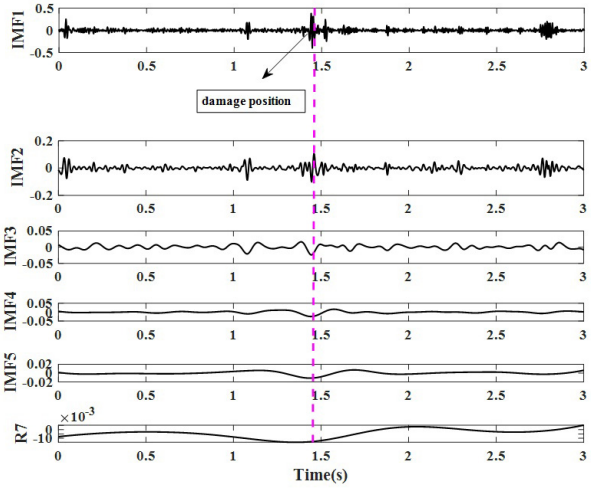

Fig. 23. CEEMD decomposition of the original IMF1.

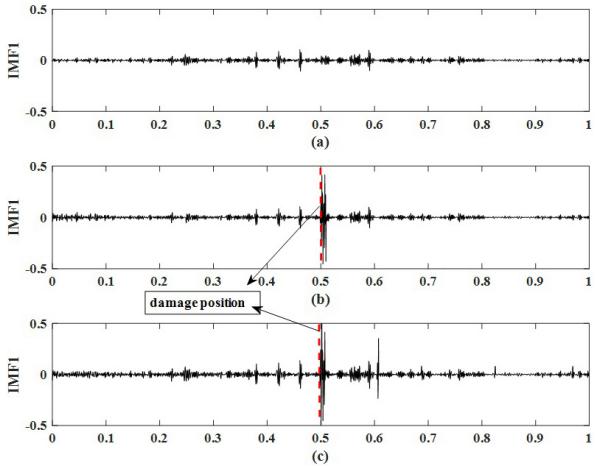

Fig. 24. (a) The identification result of undamaged; (b) $L_1 = 0.5\,L$; $d = 0.3\,h$; (c) $L_1 = 0.5\,L$; $d = 0.6\,h$.

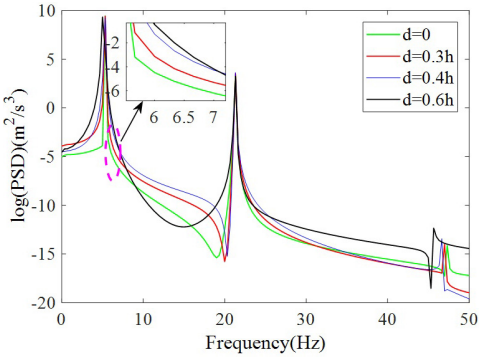

Fig. 25. PSD curve at different damage levels.

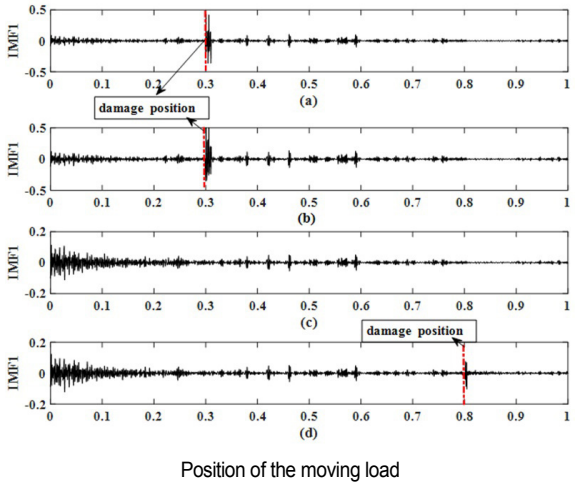

Fig. 26. Damage location identification results: (a) $L_1 = 0.3\,L$; $d = 0.4\,h$; (b) $L_1 = 0.3\,L$; $d = 0.5\,h$; (c) $L_1 = 0.2\,L$; $d = 0.4\,h$; (d) $L_1 = 0.8\,L$; $d = 0.4\,h$.

the location of the damage in the span and that the abrupt change becomes more pronounced as the degree of damage becomes greater. Fig. 25 shows the power spectrum curve corresponding to a gradually increasing depth of the crack in the span with no change in the location of the damage. It can be seen that the curve changes significantly as the depth increases. Within the selected frequency band, the curve gradually shifts upwards as the depth of damage becomes greater.

To investigate the sensitivity of the proposed method to damage at different locations, three different locations were selected for the study. As can be seen from Fig. 26, the damage is successfully identified at 0.3 L and 0.8 L. However, the damage is not identified at 0.2 L, probably due to the large anomalous signal generated when the car first entered, which results in the damage near the end of the beam not being identified.

In Fig. 27, it can be seen that the power spectrum curve (2) of the damage at the 0.2 L position is different from the no-damage curve (1), which also implies that we need to pay special attention when we are unable to determine the location of the damage using the proposed method, but there is a change in the power spectrum curve indicating that the damage occurred at the end of the beam. Comparing (4) and (6) shows

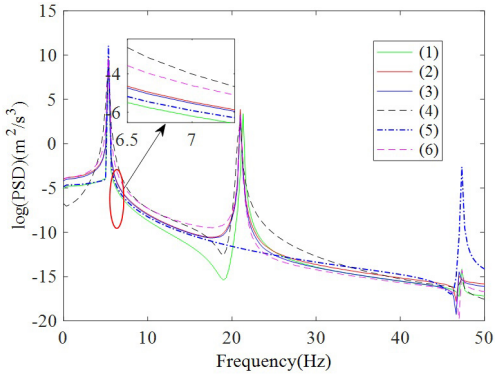

Fig. 27. PSD curve in different cases: (1) is the undamaged state (sensor no. 2); (2) $L_1 = 0.2\,L$; $d = 0.4\,h$; (3) $L_1 = 0.8\,L$; $d = 0.4\,h$; (4) $L_1 = 0.3\,L$; $d = 0.6\,h$; (5) is the undamaged state (sensor no. 3); (6) $L_1 = 0.3\,L$; $d = 0.4\,h$.

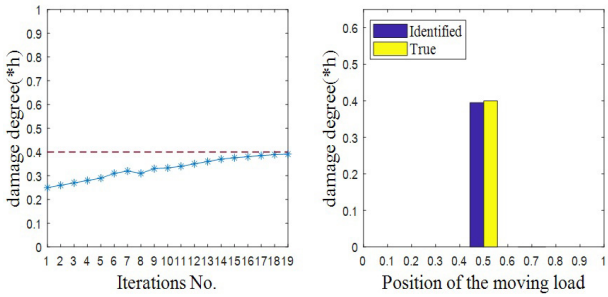

Fig. 28. Single damage identification ($L_1 = 0.5\,L$; $d = 0.4\,h$).

that the damage locations are the same, and the greater the damage, the greater the value of the power spectrum in the selected region. Curve (5) shows the power spectrum curve for the sensor at mid-span without damage. Comparing curves (1) and (5), it can be seen that the power spectrum curves for the undamaged case are different for signals collected at different locations.

It can be seen from the power spectrum curve that the frequency before and after damage changes little, but the difference in the amplitude of the curve is very large, which also shows that the power spectrum function can be used to determine the damage degree. Since the damage location has been determined, only the parameters at the damage location need to be iterated. The sensitivity of the power spectrum to the fracture depth is obtained from Eq. (13), and the damage parameters of the damaged structure are calculated from Eq. (14). After 19 iterations, the damage identification results, as shown in Fig. 28, are obtained. Both figures show that the single damage degree of the structure can be determined successfully. The detection error was 3.2 %. Similarly, the degree of damage occurring at 0.8 L can be identified in Fig. 29.

Because of the complexity of multi-damage, there are many interference signals in IMF1, so it is difficult to extract the damage feature. However, the proposed CEEMD and PSD combination method has successfully identified the single experimental damage. Next, we will continue to study the experimental

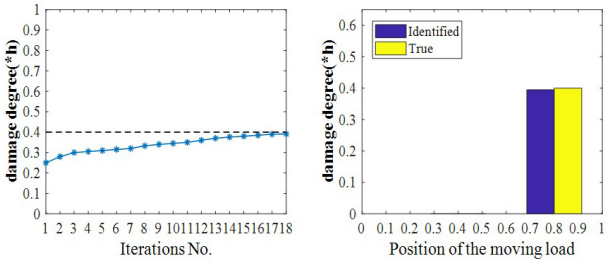

Fig. 29. Single damage identification ($L_1 = 0.8\,L$; $d = 0.4\,h$).

extraction of multi-damage features and the separation of damage-sensitive signal components.

5. Conclusions

A new approach, based on CEEMD and PSD sensitivity analysis, has been developed for monitoring the health safety of beam bridge structures under moving loads. The acceleration response is decomposed by CEEMD to obtain the natural frequency components and pseudo-frequency components of the structure. The highest-order frequency component is more sensitive to damage, so it is selected as the characteristic signal of the damage location. Damage positions are identified by direct observation of the highest-order pseudo-frequency components (IMF1), which presents an abrupt change in the damaged position. With the increase of damage degree, the abrupt change of damage location becomes more obvious, and obvious changes of left and right amplitude at the damage location can be observed in the low-frequency components. After the damage location is determined, only the power spectrum sensitivity analysis of the parameters at the damage location is needed, which greatly reduces the amount of calculation. Numerical results show that the proposed method can accurately identify the location of single and multiple damage, and the damage quantification can maintain a certain degree of accuracy, which can achieve good identification results. In addition, the method has been used to identify the single damage through experiments. The results show that the method can be used to identify single damage with a certain degree of accuracy.

Acknowledgments

The work in this paper was supported by a grant from Key Laboratory of Large Structure Health Monitoring and Control, Shijiazhuang, 050043 (Project No. KLLSHMC2107) and by a grant from Science and Technology Research Project of Higher Education of Hebei Province (Project No. QN2021025). The authors are grateful for the generous support.

Nomenclature

M : Mass matrix
C : Damping matrix
K : Stiffness matrix
H^* : Conjugate of the frequency response function
H^T : Transpose of the frequency response function
S_{ff} : Excitation spectrum
L : Beam length
B : Section width
h : Section height
ρ : Density
P : Magnitude of the moving load
V : Load speed
L_1 : Crack distance from the left end position
d : Crack depth
ρA : Mass per unit length
EI : Flexural stiffness
$w(x,t)$: Displacement of the beam
Δ : Dirac delta function
k : Stiffness of the rotational spring

References

[1] A. González and D. Hester, An investigation into the acceleration response of a damaged beam-type structure to a moving force, *J. of Sound and Vibration*, 332 (13) (2013) 3201-3217.
[2] K. Y. Wong, Instrumentation and health monitoring of cable - supported bridges, *Structural Control and Health Monitoring*, 11 (2) (2004) 91-124.
[3] E. J. OBrien and A. Malekjafarian, A mode shape-based damage detection approach using laser measurement from a vehicle crossing a simply supported bridge, *Structural Control and Health Monitoring,* 23 (10) (2016) 1273-1286.
[4] J. M. Ko and Y. Q. Ni, Technology developments in structural health monitoring of large-scale bridges, *Engineering Structures*, 27 (12) (2005) 1715-1725.
[5] W. Y. He, J He and W. X. Ren, Damage localization of beam structures using mode shape extracted from moving vehicle response, *Measurement*, 121 (2018) 276-285.
[6] H. Ouyang, Moving-load dynamic problems: A tutorial (with a brief overview), *Mechanical Systems and Signal Processing*, 25 (6) (2001) 2039-2060.
[7] R. Hou and Y. Xia, Review on the new development of vibration-based damage identification for civil engineering structures: 2010-2019, *J. of Sound and Vibration*, 491 (9) (2021) 115741.
[8] Y. C. Yang and S. Nagarajaiah, Blind identification of damage in time-varying systems using independent component analysis with wavelet transform, *Mechanical Systems and Signal Processing*, 47 (1-2) (2014) 3-20.
[9] X. Zhu, M. Cao and W. Ostachowicz, Damage identification in bridges by processing dynamic responses to moving loads: features and evaluation, *Sensors*, 19 (3) (2019).
[10] Z. Nie, J. Lin and J. Li, Bridge condition monitoring under moving loads using two sensor measurements, *Structural Health Monitoring*, 19 (3) (2019).
[11] Z. Yu and H. Xia, Bridge damage identification from moving load induced deflection based on wavelet transform and lipschitz exponent, *International J. of Structural Stability and Dynamics*, 16 (5) (2016).

[12] X. Q. Zhu and S. S. Law, Wavelet-based crack identification of bridge beam from operational deflection time history, *International Journal of Solids and Structures*, 43 (7-8) (2006) 2299-2317.
[13] N. E. Huang and Z. Shen, The empirical mode decomposition and the hilbert spectrum for nonlinear and non-stationary time series analysis, *Proceedings of the Royal Society A: Mathematical, Physical and Engineering Sciences*, 454 (1971) (1998) 903-995.
[14] Y. Lei, J. Lin and Z. He, A review on empirical mode decomposition in fault diagnosis of rotating machinery, *Mechanical Systems and Signal Processing*, 35 (2013) 108-126.
[15] Y. L. Xu and J. Chen, Structural damage detection using empirical mode decomposition: experimental investigation, *Journal of Engineering Mechanics*, 130 (11) (2004) 1279-1288.
[16] N. Roveri and A. Carcaterra, Damage detection in structures under traveling loads by hilbert-huang transform, *Mechanical Systems and Signal Processing*, 28 (2012) 128-144.
[17] Z. Wu and N. E. Huang, Ensemble empirical mode decomposition: A noise-assisted data analysis method, *Advances in Adaptive Data Analysis*, 1 (1) (2009) 1-41.
[18] H. Aied, A. Gonzáleza and D. Cantero, Identification of sudden stiffness changes in the acceleration response of a bridge to moving loads using ensemble empirical mode decomposition, *Mechanical Systems and Signal Processing*, 66-67 (2016) 314-338.
[19] J. R. Yeh, J. S. Shieh and N. E. Huang, Complementary ensemble empirical mode decomposition: A novel noise enhanced data analysis method, *Advances in Adaptive Data Analysis*, 2 (2) (2010) 135-156.
[20] Y. Niu, Y. Ye, W. Zhao and J. Shu, Dynamic monitoring and data analysis of a long-span arch bridge based on high-rate GNSS-RTK measurement combining CF-CEEMD method, *J. of Civil Structural Health Monitoring*, 11 (2021) 35-48, https://doi.org/ 10.1007 /s13349-020-00436-x.
[21] S. Liberatore and G. P. Carman, Power spectral density analysis for damage identification and location, *J. of Sound and Vibration*, 274 (3-5) (2004) 761-776.
[22] Y. Fang, X. Liu, J. Xing, Z. Li and Y. Zhang, Substructure damage identification based on sensitivity of power spectral density, *J. of Sound and Vibration,* 545 (2013) 117451.
[23] B. Zhang, Y. Qian, Y. Wu and Y. B. Yang, An effective means for damage detection of bridges using the contact-point response of a moving test vehicle, *J. of Sound and Vibration*, 419 (2018) 158-172.

Youliang Fang received his Ph.D. in aircraft design from Beijing University of Aeronautics and Astronautics in 1999. He is now a Professor at Hebei University. His research interests include structural health monitoring, structural performance evaluation, structural vibration and control, structural construction simulation and control, structural disaster simulation.

Jie Xing received the B.E. from Xi'an University of Architecture and Technology, China, in 2020. Now he is studying for a Master's at Hebei University. His current research interest is structural damage identification.

Ying Zhang is lecturer of College of Civil Engineering and Architecture, Hebei University. She received her Ph.D. from the School of Energy Power and Mechanical Engineering, North China Electric Power University. Her research interests include structural health monitoring of bridge engineering and building structure, mechanics and vibration.